Mixed convective radiative flow of vicoelastic liquid subject to space dependent internal heat source and chemical reaction

Tasawar Hayat [a,b], Ikram Ullah [a] [1], Ahmed Alsaedi [b] and Bashir Ahmad [b]

[a] Department of Mathematics, Quaid-I-Azam University 45320, Islamabad 44000, Pakistan

[b] Nonlinear Analysis and Applied Mathematics (NAAM) Research Group, Department of Mathematics, Faculty of Science, King Abdulaziz University P. O. Box 80203, Jeddah 21589, Saudi Arabia

Abstract: Present study addresses Soret and Dufour effects in mixed convection MHD flow of viscoelastic liquid with chemical reaction. Flow induced by an exponential stretching sheet is addressed in the presence of magnetic field. Energy expression is modelled by exponential space dependent internal heat source, thermal radiation and convective condition. Relevant problems are modelled by employing boundary layer concept. The partial differential systems are reduced to ordinary differential systems. Resultsnt problem is solved by homotopic technique. Physical insight of results is arranged by graphs and tables.

Keywords: Viscoelastic liquid; Exponential based heat source; Mixed convection; Chemical reaction.

Introduction

Liquid flow over a stretched surface has been attracted by the engineers, numerical simulists and modelers. It is due to its vast applications in the manufacturing process and polymer industry comprising spinning of filaments, wire drawing, hot rolling, production of crystal growing fibers, processing of food stuffs, paper production, rapid spray cooling, continues casting, cooling of microelectronics and glass blowing. Crane [1] inspected the boundary-layer flow of an incompressible viscous fluid over a linear stretching sheet. He obtained similarity solution in closed form. Since then, many researchers [2-8] provided their research contributions via various concept of stretching surfaces. However in fact the stretching of a plastic sheet may not essentially be linear. The characteristics of flow and heat transfer by an exponentially stretched surface is important for thinning and annealing of copper wires, food, paper and plastic processes. The final product depends critically on rate of heat transfer and stretching. Both kinematics of cooling or simultaneous heating and stretching have a crucial affect on the nature of final product [9]. Magyari and Keller [10] examined the flow due to an exponentially stretching sheet. They studied the heat transfer aspects in the case where the wall temperature varies exponentially from the leading edge. Viscous dissipation in mixed convective flow by an exponentially stretching surface is studied by Partha et al. [11]. It is found that velocity enhances for both mixed convection and viscous dissipation. Sajid and Hayat [12] explored radiation in flow by an exponentially stretching surface. Flow of magneto second grade nanoliquid persuaded by an exponentially stretching sheet discussed by Hayat et al. [13].

The respective mass/energy fluxes can be achieved by taking gradients of temperature/concentration. Thermal-diffusion (Soret effect) is generated because of temperature gradient while diffusion-thermo (Dufour effect) occurred due to concentration gradient. Such aspects have great implementation in area of chemical engineering and geosciences. Soret effect

[1]Corresponding author. Tel.: +92-51 90642172.
email address: ikram020@yahoo.com

can be seen in solar ponds, micro-structure and the biological systems of the world oceans. Thermal-diffusion is also utilized in process of isotope separation and in mixture between gases with small molecular weight (He, H_2) and of medium molecular weight (air, N_2). Related analysis in this direction have been mentioned by the studies [14-18].

Excessive heat generation is a serious issue in engineering applications like nuclear power plants, concrete industry, computer processors and inside of earth. Effective heat transfer can drastically improve the effectiveness in such cases. There is most likely that heat transfer is very valuable in dilution technique, dialysis, oxygenation and hyperthermia. Tissue engineering uses thermal excursion to selectively destroy tissues and cells. All these applications require heat transfer in the most proficient way by utilizing both free and forced convection which frequently supports mass transfer too. Heat and mass transfer through mixed convection is noticeable in processes like food solidification, diffusion of nutrients, reverse osmosis, cooling of nuclear reactors, float glass production cell separation, chemical waste management, cooling of combustion chamber wall in a gas defroster and turbine system. Many researchers admits the importance of involvement of mixed convection. Mixed convection in MHD viscoelastic fluid flow over a porous stretching sheet is analytically elaborated by Turkyilmazoglu [19]. Mixed convective boundary layer flow over a convectively heated sheet is addressed by Grosan et al. [20]. MHD mixed convective flow by an inclined porous plate with slip effect is discussed by Das et al. [21]. Imtiaz et al. [22] studied mixed convective nanofluid flow with Newtonian heating. Hayat et al. [23] studied mixed convection in 3D flow of Sisko nanoliquid. Further importance of thermal radiation is prevalent in the industrial and space technology process at vary high temperature. Furnace design, plasma physics, space craft re-entry and propulsion system, satellites, nuclear plants etc are examples of such processes. In general radiation along with the free and forced convective flows is of crucial importance in space technology and high temperature processes. Human body sustains suitable temperature by considering these two procedures. Few studies for thermal radiation in the presence of mixed convection are given through refs. [24-28].

Here our motivation is to assess the outcome of exponential heat source in flow of viscoelastic liquid by an exponentially moving surface. Few investigators in the past only utilized exponential heat source [29-31]. There is no analysis available yet that looks flow of viscoelastic liquid with such aspect. Additionally we accounted radiation, thermal-diffusion and diffusion-thermo (cross-diffusion) and chemical reaction. The governing problems are achieved via boundary layer assumptions. Homotopic approach [32-43] is employed for the solutions of non-dimensional governing problems. Physics of sundry variables are studied graphically and for tabulated values.

Problems development

Consider 3D mixed convection flow of an incompressible viscoelastic liquid. Exponentially stretching sheet induces the flow. Applied magnetic field is imposed along $z-$axis. Small magnetic Reynolds number is accounted. The laminar flow is restricted in the domain $z>0$. Heat and mass transfer characteristics have been adopted when both Soret and Dufour effects are present. Additionally exponentially heat source and chemical reaction are addressed. Radiation is entertained in the energy expression. Moreover the respective sheet and ambient liquid temperatures and concentrations are designated through (T_f and T_∞) and (C_w and C_∞). Keeping the aforesaid assumptions in mind, the governing problems are

$$\frac{\partial u}{\partial x}+\frac{\partial v}{\partial y}+\frac{\partial w}{\partial z}=0, \tag{1}$$

$$u\frac{\partial u}{\partial x}+v\frac{\partial u}{\partial y}+w\frac{\partial u}{\partial z}=\nu\frac{\partial^2 u}{\partial z^2}-k_0\left(\begin{array}{c} u\frac{\partial^3 u}{\partial x\partial z^2}+w\frac{\partial^3 u}{\partial z^3}-\frac{\partial u}{\partial x}\frac{\partial^2 u}{\partial z^2} \\ -\frac{\partial u}{\partial z}\frac{\partial^2 w}{\partial z^2}-2\frac{\partial u}{\partial z}\frac{\partial^2 u}{\partial x\partial z}-2\frac{\partial w}{\partial z}\frac{\partial^2 u}{\partial z^2}\end{array}\right) \\ -\frac{\sigma B_0^2}{\rho}u+g(\beta_T(T-T_\infty)+\beta_C(C-C_\infty)), \tag{2}$$

$$u\frac{\partial v}{\partial x}+v\frac{\partial v}{\partial y}+w\frac{\partial v}{\partial z}=\nu\frac{\partial^2 v}{\partial z^2}-k_0\left(\begin{array}{c} v\frac{\partial^3 v}{\partial x\partial z^2}+w\frac{\partial^3 v}{\partial z^3}-\frac{\partial v}{\partial y}\frac{\partial^2 v}{\partial z^2} \\ -\frac{\partial v}{\partial z}\frac{\partial^2 w}{\partial z^2}-2\frac{\partial v}{\partial z}\frac{\partial^2 v}{\partial x\partial z}-2\frac{\partial w}{\partial z}\frac{\partial^2 v}{\partial z^2}\end{array}\right) \\ -\frac{\sigma B_0^2}{\rho}v, \tag{3}$$

$$u\frac{\partial T}{\partial x}+v\frac{\partial T}{\partial y}+w\frac{\partial T}{\partial z}=\alpha_m\frac{\partial^2 T}{\partial z^2}+\frac{Dk_T}{c_s c_p}\frac{\partial^2 C}{\partial z^2}-\frac{1}{\rho c_p}\frac{\partial q_r}{\partial z} \\ +Q_0\frac{(T_w-T_\infty)}{\rho c_p}\exp\left(-\left(\frac{U_0}{2\nu L}\right)^{1/2}e^{\frac{x+y}{2L}}z\right), \tag{4}$$

$$u\frac{\partial C}{\partial x}+v\frac{\partial C}{\partial y}+w\frac{\partial C}{\partial z}=D\frac{\partial^2 C}{\partial z^2}+\frac{Dk_T}{T_m}\frac{\partial^2 T}{\partial z^2}-K_m(C-C_\infty). \tag{5}$$

$$u=U_w,\ v=V_w,\ w=0,\ k\frac{\partial T}{\partial z}=h_f(T_f-T),\ C=C_w \text{ at } z=0, \tag{6}$$

$$u\to 0,\ v\to 0,\ T\to T_\infty,\ C\to C_\infty \text{ as } z\to\infty, \tag{7}$$

where $(u,\ v,\ w)$ denote the respective velocity components parallel to $(x,\ y,\ z)$, $k_0=-\frac{\alpha_1}{\rho}$ the elastic parameter with $k_0>0$ represents elastico-visous liquid, $k_0<0$ for second grade fluid and $k_0=0$ for viscous liquid, α_1 the normal stress moduli, Q_0 the heat generation/absorption variable, $\nu=\mu/\rho$ the kinematic viscosity, ρ the density, g the acceleration due to gravity, μ the dynamic viscosity, β_C the coefficient of solutal expansion, T the temperature, β_T the coefficient of thermal expansion, α_m the thermal diffusivity, k_T the thermal-diffusion, D the diffusion coefficient, c_p the specific heat, T_m the fluid mean temperature, q_r the radiative heat flux, C the concentration, c_s the concentration susceptibility, K_m the chemical reaction rate and h_f the convective heat transfer coefficient. This analysis presumes that surface stretching velocities, wall temperature and concentration are

$$U_w=U_0 e^{\frac{x+y}{L}},\ V_w=V_0 e^{\frac{x+y}{L}},\ T_w=T_f=T_\infty+T_0 e^{\frac{A(x+y)}{2L}},\ C_w=C=C_\infty+C_0 e^{\frac{B(x+y)}{2L}}, \tag{8}$$

where U_0, V_0, T_0 and C_0 are the constants, A is the temperature exponent, B is the concentration exponent and L is the reference length. Through Rosseland's approximation the expression for radiative heat flux q_r is

$$q_r=-\frac{4\sigma_1}{3m^{**}}\frac{\partial(T^4)}{\partial y}=-\frac{16\sigma^{**}T_\infty^3}{3m^{**}}\frac{\partial^2 T}{\partial z^2}, \tag{9}$$

in which σ^{**} shows the Stefan-Boltzman and m^{**} designates the coefficient of mean absorption. Invoking Eq. (9) the energy equation can be converted to the form

$$
\left.\begin{aligned}
&u\frac{\partial T}{\partial x}+v\frac{\partial T}{\partial y}+w\frac{\partial T}{\partial z}=\alpha_m\frac{\partial^2 T}{\partial z^2}+\frac{Dk_T}{c_s c_p}\frac{\partial^2 C}{\partial z^2}+\frac{16\sigma_1 T_\infty^3}{3m\rho c_p}\frac{\partial^2 T}{\partial z^2}\\
&\qquad +Q_0\frac{(T_w-T_\infty)}{\rho c_p}\exp\left(-\left(\frac{U_0}{2\nu L}\right)^{1/2}e^{\frac{x+y}{2L}}z\right),
\end{aligned}\right\} \tag{10}
$$

The dimensionless variables are taken in the forms

$$
\begin{aligned}
&u=U_0 e^{\frac{x+y}{L}}f'(\eta),\ v=U_0 e^{\frac{x+y}{L}}g'(\eta),\ w=-\left(\frac{\nu U_0}{2L}\right)^{1/2}e^{\frac{x+y}{2L}}\left(f+\eta f'+g+\eta g'\right),\\
&T=T_\infty+T_0 e^{\frac{A(x+y)}{2L}}\theta(\eta),\ C=C_\infty+C_0 e^{\frac{B(x+y)}{2L}}\phi(\eta),\ \eta=\left(\frac{U_0}{2\nu L}\right)^{1/2}e^{\frac{x+y}{2L}}z.
\end{aligned} \tag{11}
$$

Equation (1) is identically satisfied while the Eqs. $(2)-(8)$ and Eq. (10) give

$$
\left.\begin{aligned}
&f'''+(f+g)f''-2(f'+g')f'+K\begin{pmatrix}6f'''f'+(3g''-3f''+\eta g''')f''\\+(4g'+2\eta g'')f'''-(f+g+\eta g')f''''\end{pmatrix}\\
&\qquad -M^2 f'+2\lambda(\theta+N\phi)=0,
\end{aligned}\right\} \tag{12}
$$

$$
\left.\begin{aligned}
&g'''+(f+g)g''-2(f'+g')g'+K\begin{pmatrix}6g'''g'+(3f''-3g''+\eta f''')g''\\+(4f'+2\eta f'')g'''-(f+g+\eta f')g''''\end{pmatrix}\\
&\qquad -M^2 g'=0,
\end{aligned}\right\} \tag{13}
$$

$$
\left(1+Rd\right)\theta''+\Pr[\left(f+g\right)\theta'-A\left(f'+g'\right)\theta+D_f\phi''+\delta\exp(-\eta)]=0, \tag{14}
$$

$$
\phi''+Sc[\left(f+g\right)\phi'-B\left(f'+g'\right)\phi+Sr\theta''-\gamma_1\phi]=0, \tag{15}
$$

$$
f=0,\ g=0,\ f'=1,\ g'=\alpha,\ \theta'=-\gamma(1-\theta(0)),\ \phi'=1 \text{ at } \eta=0, \tag{16}
$$

$$
f'\to 0,\ g'\to 0,\ \theta\to 0,\ \phi\to 0 \text{ as } \eta\to\infty. \tag{17}
$$

Here λ shows mixed convection variable, K dimensionless viscoelastic parameter, M magnetic parameter, δ heat source parameter, N buoyancy ratio, Gr Grashof number, Re Reynold number, α ratio parameter, Rd radiation parameter, D_f Dufour number, $\Pr$ Prandtl number, Sr Soret number, Sc Schmidt number, γ Biot number due to temperature and γ_1 chemical reaction parameter. These quantities have values

$$
\left.\begin{aligned}
&\lambda=\frac{Gr}{\mathrm{Re}^2},\ N=\frac{\beta_C(C_w-C_\infty)}{\beta_T(T_w-T_\infty)},\ Gr=\frac{g\beta_T(T_w-T_\infty)}{\nu^2},\ \mathrm{Re}=\frac{U_w L}{\nu}\ \alpha=\frac{V_0}{U_0},\ K=\frac{k_0 U_w}{2\nu L},\\
&\Pr=\frac{\nu}{\alpha_m},\ Rd=\frac{16\sigma_1 T_\infty^3}{3km},\ D_f=\frac{Dk_T}{c_s c_p \nu}\frac{(C_w-C_\infty)}{(T_w-T_\infty)},\ Sc=\frac{\nu}{D},\ Sr=\frac{Dk_T}{T_m \nu}\frac{(T_w-T_\infty)}{(C_w-C_\infty)},\\
&\gamma=\frac{h}{k}\sqrt{\frac{2\nu L}{U_w}},\ \gamma_1=\frac{K_m L}{U_0},\ \delta=\frac{Q_0 L}{U_0\rho c_p},\ M^2=\frac{2\sigma B_0^2 L}{\rho U_w}.
\end{aligned}\right\} \tag{18}
$$

Expressions for local Nusselt number (Nu_x) and Sherwood (Sh_x) numbers are stated as

$$
Nu_x=\frac{xq_w}{k\left(T_w-T_\infty\right)}+(q_r)_w,\ Sh_x=\frac{xj_w}{D\left(C_w-C_\infty\right)}, \tag{19}
$$

where

$$
q_w=-k\left(\frac{\partial T}{\partial z}\right)_{z=0},\ j_w=-D\left(\frac{\partial C}{\partial z}\right)_{z=0}. \tag{20}
$$

Eq. (19)-(20) in non-dimensional form gives

$$\left(\frac{\mathrm{Re}_x}{2}\right)^{-1/2} Nu_x = -\frac{x}{L}\left(1+Rd\right)\theta'(0), \tag{21}$$

$$\left(\frac{\mathrm{Re}_x}{2}\right)^{-1/2} Sh_x = -\frac{x}{L}\phi'\left(0\right), \tag{22}$$

where $\mathrm{Re} = U_w L/\nu$ defines the Reynolds number.

Analysis of series solutions

The initial approximations (f_0, g_0, θ_0, ϕ_0) and operators ($\bar{\mathbf{L}}_f$, $\bar{\mathbf{L}}_g$, $\bar{\mathbf{L}}_\theta$, $\bar{\mathbf{L}}_\phi$) are

$$\left.\begin{array}{l} f_0(\eta) = 1 - e^{-\eta}, \quad g_0(\eta) = \alpha(1 - e^{-\eta}) \\ \theta_0(\eta) = \frac{\gamma}{1+\gamma} e^{-\eta}, \quad \phi_0(\eta) = \frac{\gamma_1}{1+\gamma_1} e^{-\eta}, \end{array}\right\} \tag{23}$$

$$\left.\begin{array}{l} \bar{\mathbf{L}}_f = f''' - f', \quad \bar{\mathbf{L}}_g = g''' - g' \\ \bar{\mathbf{L}}_\theta = \theta'' - \theta, \quad \bar{\mathbf{L}}_\varphi = \phi'' - \phi, \end{array}\right\} \tag{24}$$

with

$$\left.\begin{array}{l} \bar{\mathbf{L}}_f\left[\beta_1^{**} + \beta_2^{**} e^{\eta} + \beta_3^{**} e^{-\eta}\right] = 0, \quad \bar{\mathbf{L}}_g\left[\beta_4^{**} + \beta_5^{**} e^{\eta} + \beta_6^{**} e^{-\eta}\right] = 0, \\ \bar{\mathbf{L}}_\theta\left[\beta_7^{**} e^{\eta} + \beta_8^{**} e^{-\eta}\right] = 0, \quad \bar{\mathbf{L}}_\phi\left[\beta_9^{**} e^{\eta} + \beta_{10}^{**} e^{-\eta}\right] = 0 \end{array}\right\} \tag{25}$$

in which β_i^{**} $(i = 1-10)$ depict the constants.

Here it is desired to achieve the admissible ranges of embedding variables for convergence of series solutions. For such intention, we have sketched the $\hbar$ curves (see Figs. 1 and 2). Clearly these Figs. depict that acceptable values of these embedding variables are $-0.65 \le \hbar_f \le -0.09$, $-0.64 \le \hbar_g \le -0.01$, $-1.03 \le \hbar_\theta \le 0.1$ and $-0.98 \le \hbar_\phi \le 0.1$.

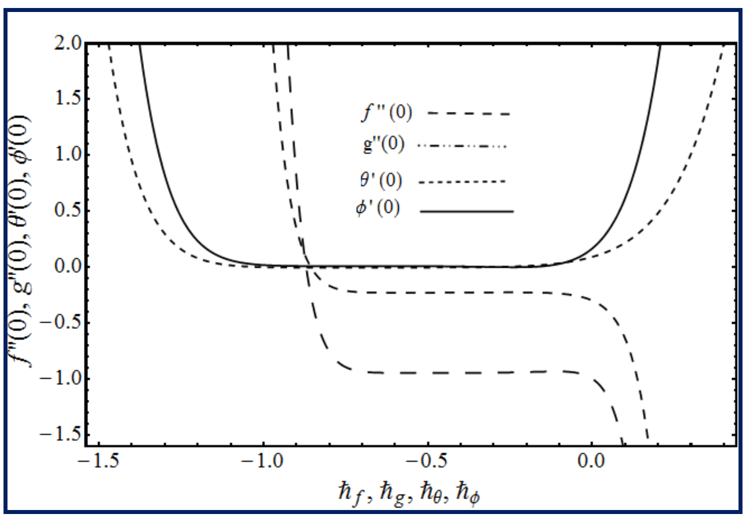

Fig. 1: $\hbar$-curves for $f(\eta), g(\eta), \theta(\eta)$ and $\phi(\eta)$.

Discussion

Main emphasis here is given to address the salient feature of influential parameters on velocities, temperature and concentration. The responses of Nusselt and Sherwood numbers for distinct values of interesting variables are examined (see Table 1). Aspects of α on $f'(\eta)$ and $g'(\eta)$

are portrayed in Figs. 2 and 3. Here velocity components $f'(\eta)$ and $g'(\eta)$ show reverse trend when α is enhanced. Physically when α increases from zero then lateral surface begins to expand in the $y-$direction and it shrink in $x-$direction. Thus $g'(\eta)$ increases while the velocity components $f'(\eta)$ diminishes. Influences of λ on velocity profiles $f'(\eta)$ and $g'(\eta)$ are displayed in Figs. 4 and 5. It is clearly shown that $f'(\eta)$ enhances by increasing λ. In fact viscous forces are less effective rather then buoyancy forces. Opposite feature of $g'(\eta)$ is seen for higher λ. Figs. 6 and 7 are sketched to visualize the behavior of N on $f'(\eta)$ and $g'(\eta)$. Here larger N result for an increment in $f'(\eta)$. For larger N both $g'(\eta)$ and momentum layer decayed. Curves of dimensionless $\theta(\eta)$ with change in M is elucidated in Fig. 8. This Fig. reveals that $\theta(\eta)$ marginally increases as M is enhanced. It is well known fact that magnetic field intensity tends to produced drag force which resists the liquid motion and ultimately the thermal field is elevated. Fig. 9 is drawn to see the characteristics of δ on $\theta(\eta)$. It is found that $\theta(\eta)$ is augmented for larger δ. Fig. 10 is sketched to analyze behavior of Biot number γ on $\theta(\eta)$. It is concluded that $\theta(\eta)$ and related layer thickness are enhanced for larger γ. Fig. 11 demonstrates to analyze the behavior of Rd on temperature $\theta(\eta)$ It is reported that $\theta(\eta)$ is enhanced for higher Rd. Physically an increment in radiation promotes the heat flux which corresponds to rise in $\theta(\eta)$. Fig. 12 elucidates that an increase in $\Pr$ decays the thermal field. The fluid with higher $\Pr$ is more viscous. The fluid with a higher viscosity has a lower temperature while the fluid with lower viscosity has higher temperature. Thus an increase in $\Pr$ leads to diminish $\theta(\eta)$. Impact of Sr on $\theta(\eta)$ is depicted in Fig. 13. There is reduction in $\theta(\eta)$ for higher Sr. Temperature identifies increasing nature with intensity of D_f (see Fig. 14). In fact D_f is involved in energy expression by concentration gradient. Therefore $\theta(\eta)$ is enhanced with higher concentration gradient. Figs. 15 and 16 are drawn to see the impacts of γ_1 for generative $(\gamma_1 < 0)$ and destructive $(\gamma_1 > 0)$ chemical reactions for $\phi(\eta)$. Concentration field $\phi(\eta)$ reduces with increment in destructive chemical reaction $(\gamma_1 > 0)$ while it enhances in case of $(\gamma_1 < 0)$. Behavior of Sc on $\phi(\eta)$ is presented in Fig. 17. Schmidt number is the ratio of momentum diffusivity to the mass diffusivity higher Sc lead to decay in mass diffusivity which in turn declines the concentration field. Fig. 18 portrays the variation in $\phi(\eta)$ for various Sr. Here $\phi(\eta)$ is an increasing function of Sr. Fig. 19 designates that higher Dufour number D_f enhances the concentration and its related boundary layer thickness. Tables 1 perceives numerical data of Nusselt and Sherwood numbers Rd, γ, $\gamma 1$, Sr, D_f and δ. Here we concluded that Nusselt number enhances for Rd, γ, and Sr. It is also noted that Sherwood numbers decay via γ, δ and Sr.

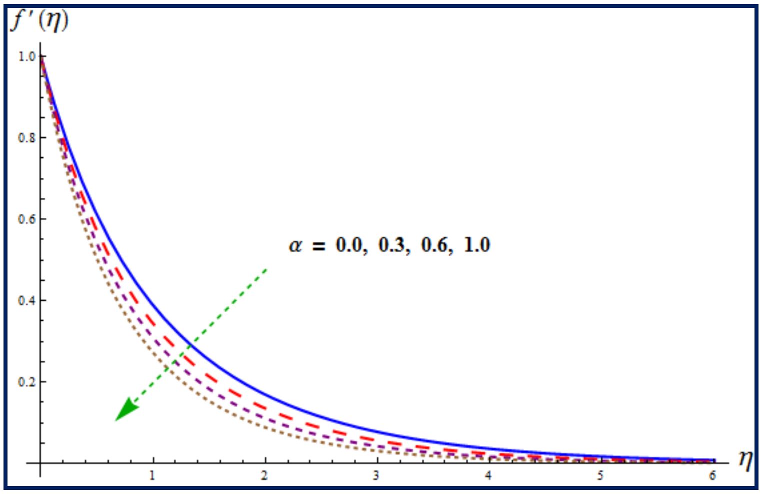

Fig. 2. Impact of $f'(\eta)$ via α.

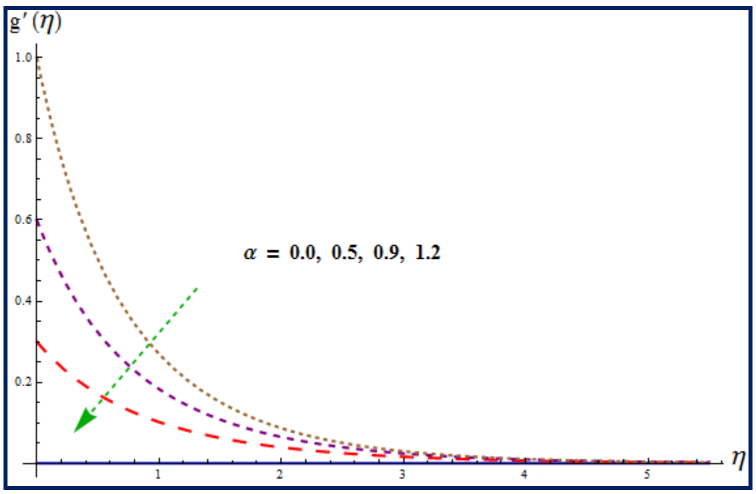

Fig. 3. Impact of $g'(\eta)$ via α.

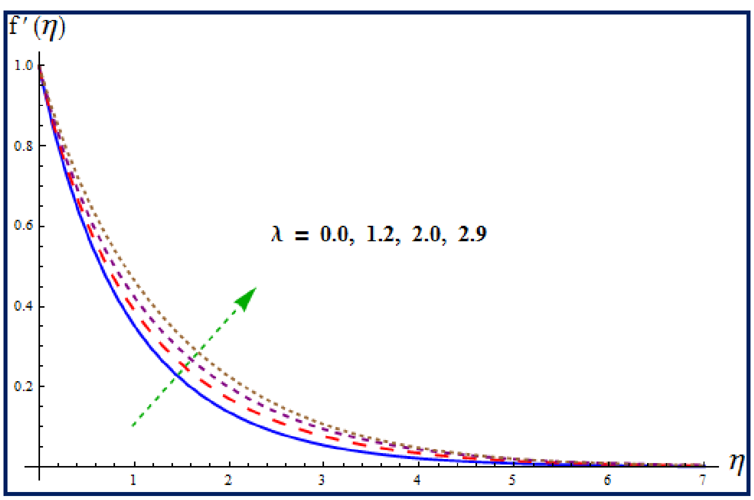

Fig. 4. Impact of $f'(\eta)$ via λ.

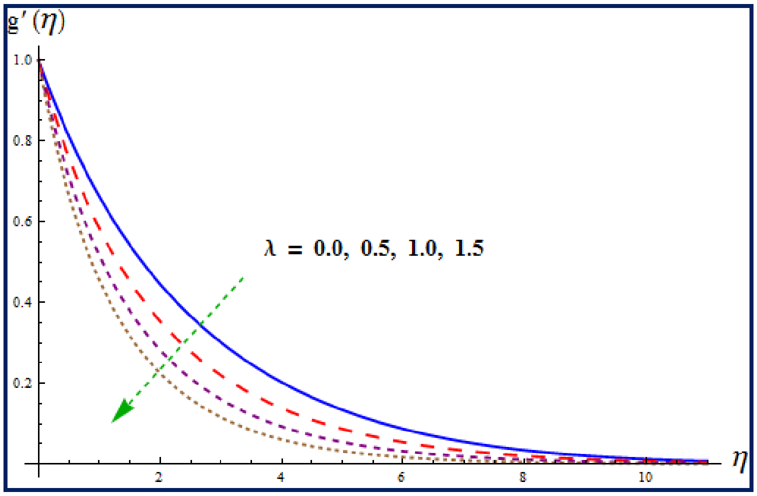

Fig. 5. Impact of $g'(\eta)$ via λ.

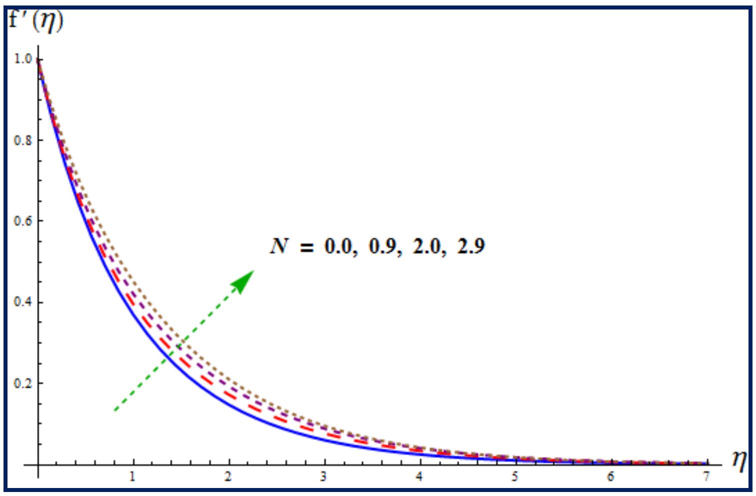

Fig. 6. Impact of $f'(\eta)$ via N.

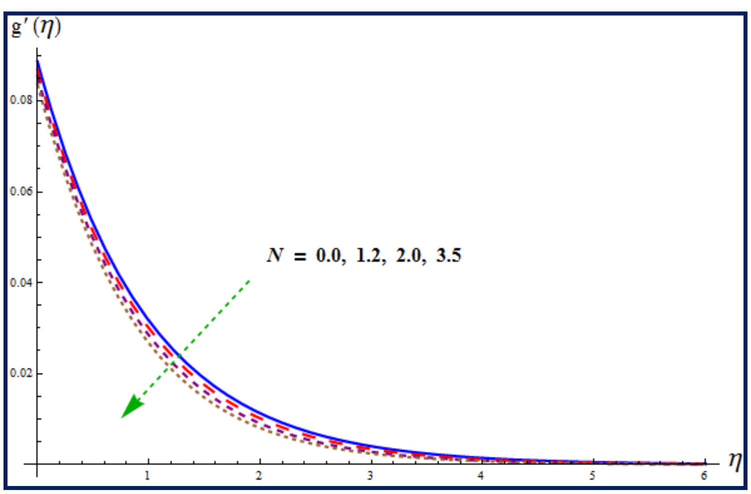

Fig. 7. Impact of $g'(\eta)$ via N.

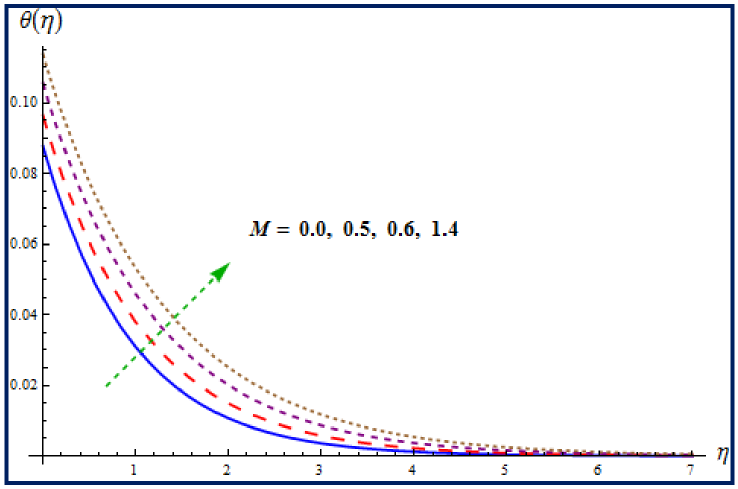

Fig. 8. Impact of $\theta(\eta)$ via M .

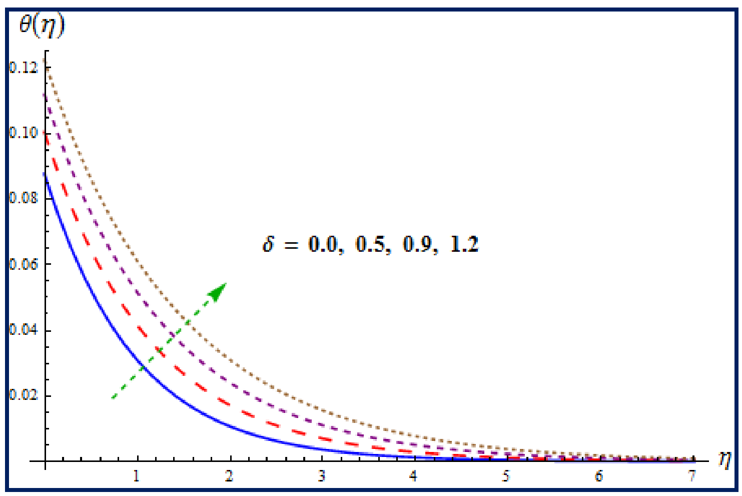

Fig. 9. Impact of $\theta(\eta)$ via δ .

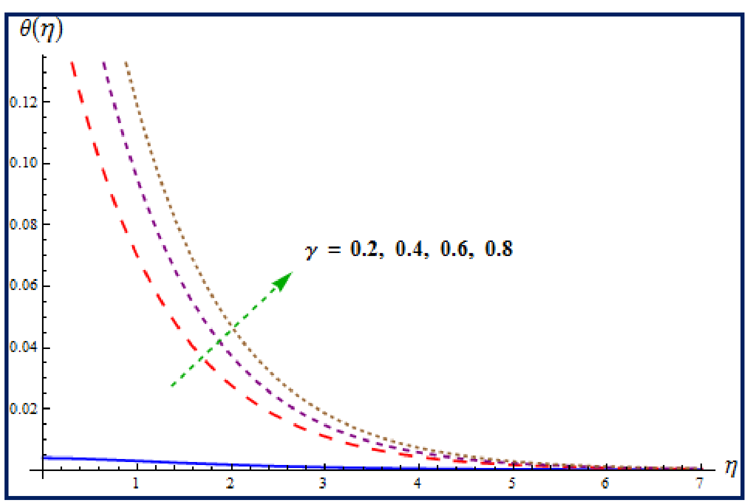

Fig. 10. Impact of $\theta(\eta)$ via γ .

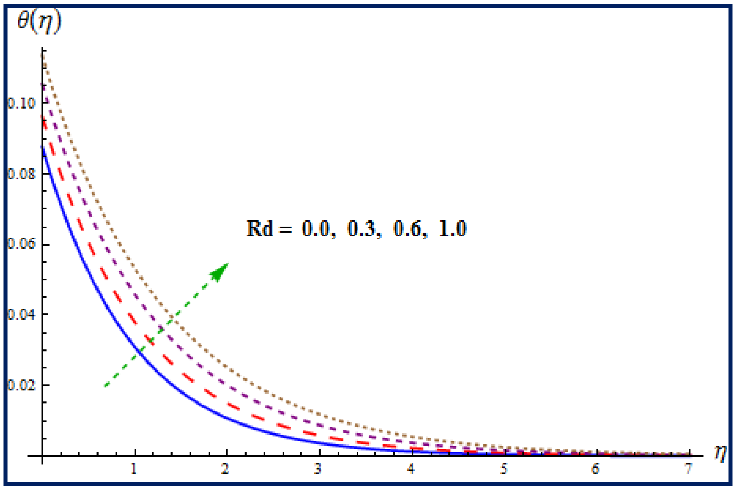

Fig. 11. Impact of $\theta(\eta)$ via Rd .

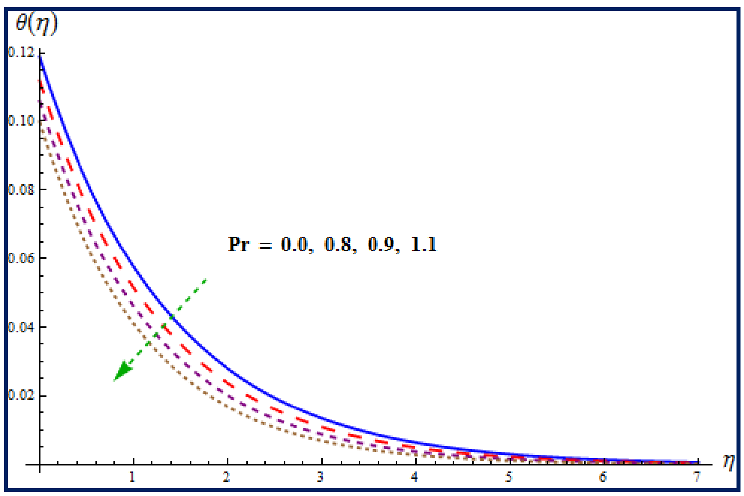

Fig. 12. Impact of $\theta(\eta)$ via Pr .

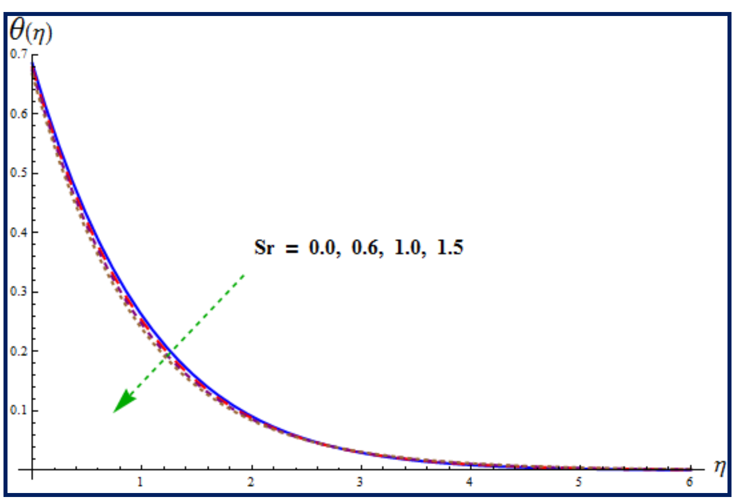

Fig. 13. Impact of $\theta(\eta)$ via Sr .

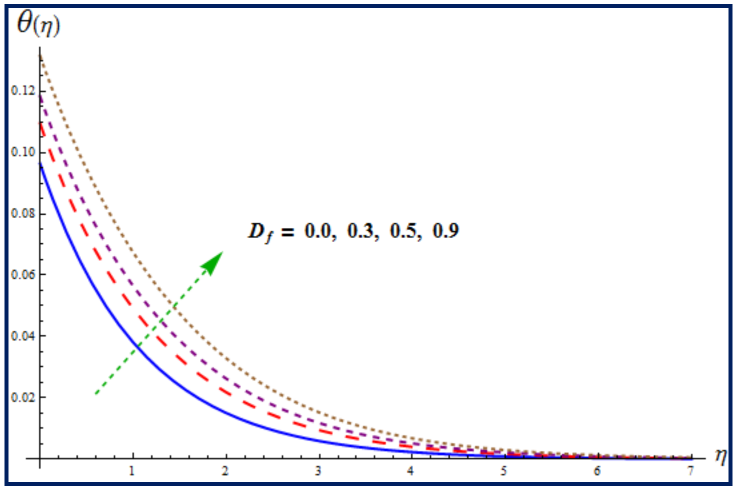

Fig. 14. Impact of $\theta(\eta)$ via D_f.

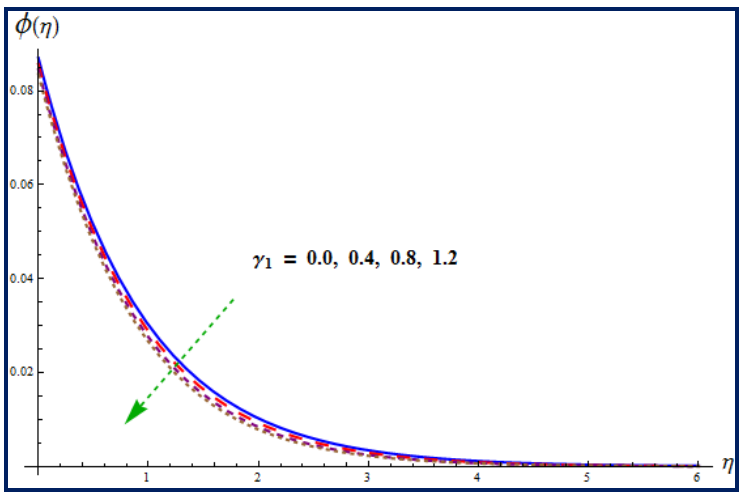

Fig. 15. Impact of $\phi(\eta)$ via $(\gamma_1 \geq 0)$.

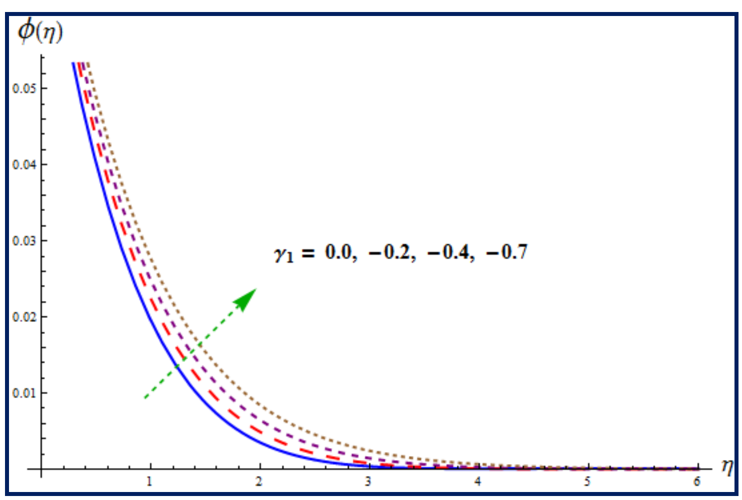

Fig. 16. Impact of $\phi(\eta)$ via $(\gamma_1 \leq 0)$.

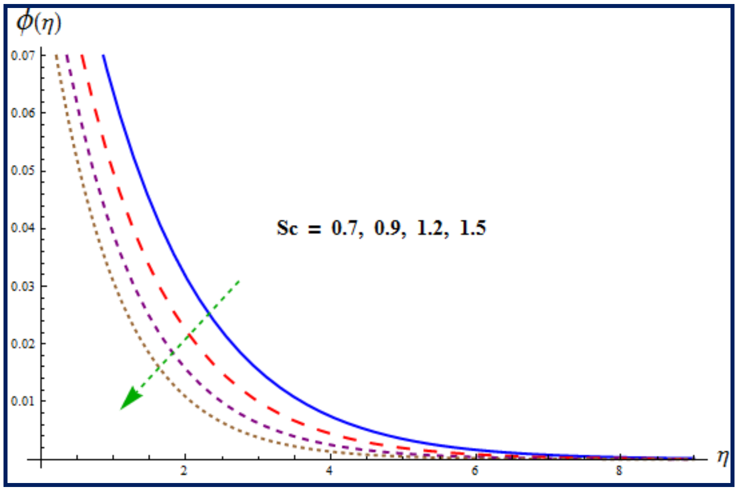

Fig. 17. Impact of $\phi(\eta)$ via Sc.

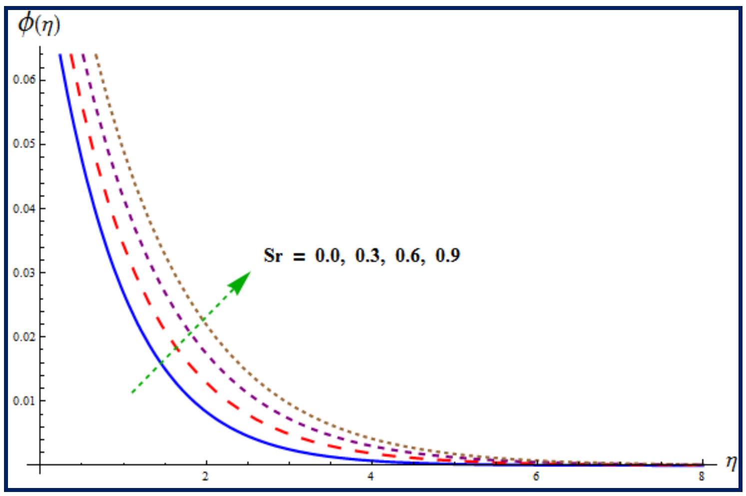

Fig. 18. Impact of $\phi(\eta)$ via Sr.

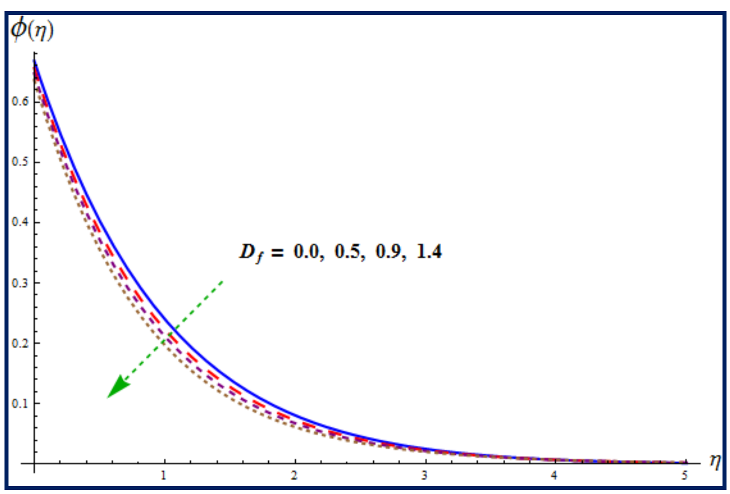

Fig. 19. Impact of $\phi(\eta)$ via D_f.

Table 1: Numerical data of surface heat transfer rate $-(1+Rd)\theta'(0)$ and surface mass transfer rate $-\phi'(0)$ for δ, Rd γ_1 γ, Sr and Df when other parameters are fixed.

δ	γ	Rd	γ_1	Sr	D_f	$(1+Rd)\theta'(0)$	$\phi'(0)$
0.0						0.10054	0.09181
0.3						0.10018	0.09151
1.0						0.09999	0.09150
	0.4					0.38052	0.08945
	1.0					0.50124	0.08420
	1.4					0.71584	0.07760
		0.0				0.09430	0.08964
		0.3				0.12612	0.90024
		0.6				0.75010	0.42019
			0.4			0.14561	0.93047
			0.8			0.14562	1.23450
			1.2			0.14563	1.34501
				0.0		0.09986	0.09171
				0.5		0.09990	0.08943
				0.9		0.09993	0.08805
					0.0	0.10037	0.09124
					0.4	0.09787	0.09129
					1.2	0.09636	0.09132

Closing remarks

Here we addressed the effects of Soret-Dufour and exponential space dependent internal heat source on MHD flow of viscoelastic liquid towards an exponentially stretched surface. Key results can be highlighted in the following bullets:

- Similar feature of velocity profiles are noticed for larger λ and N.
- Radiation and heat source variables improves the temperature field.
- Temperature is an increasing function of M.
- Features of Sr and Df on temperature and concentration are quite reverse.
- Surface heat and mass transfer rates are augmented via δ.

References

[1] L.J. Crane, Flow past a stretching plate, Z. Angew Math. Phys., 21 (1970) 645.

[2] P.S. Gupta and A.S. Gupta, Heat and mass transfer on a stretching sheet with suction and blowing, Can. J. Chem. Eng., 55 (1977) 744.

[3] C.K. Chen and M.I Char, Heat transfer of a continuous stretching surface with suction or blowing, J. Math. Anal. Appl., 135 (1988) 568.

[4] I. Pop and T.Y. Na, Unsteady flow past a stretching sheet, Mech. Res. Commun., 23 (1996) 413.

[5] S. Kazem, M. Shaban and S. Abbasbandy, Improved an alytical solutions to a stagnation-point flow past a porous stretching sheet with heat generation, J. Frankl Inst., 348 (2011) 2044.

[6] T. Hayat, I. Ullah, A. Alsaedi and M. Farooq, MHD flow of Powell-Eyring nanofluid over a non-linear stretching sheet with variable thickness, Results in Phys., 7 (2017) 189-196.

[7] M. Hussain, M. Ashraf, S. Nadeem and M. Khan, Radiation effects on the thermal boundary layer flow of a micropolar fluid towards a permeable stretching sheet, J. Frankl Inst., 350 (2013) 194.
[8] T. Hayat, I. Ullah, A. Alsaedi and S. Asghar, Flow of magneto Williamson nanoliquid towards stretching sheet with variable thickness and double stratification, Radiat. Phys. Chem., (2018), Radiat. Phys. Chem., 152 (2018) 151--157.
[9] D. Pal, Mixed convection heat transfer in the boundary layers on an exponentially stretching surface with magnetic field, Appl. Math. Comput., 217 (2010) 2356.
[10] E. Magyari and B. Keller, Heat and mass transfer in the boundary layers on an exponentially stretching continuous surface, J. Phys. Appl. Phys., 32 (1999) 577.
[11] M. K. Partha, P.V.S.N. Murthy and G.P. Rajasekhar, Effect of viscous dissipation on the mixed convection heat transfer from an exponentially stretching surface, Heat Mass Transf., 41 (2005) 306.
[12] M. Sajid and T. Hayat, Influence of thermal radiation on the boundary layer flow due to an exponentially stretching sheet, Int .Commun. Heat Mass Transf., 35 (2008) 347.
[13] T. Hayat, I. Ullah, T. Muhammad and A. Alsaedi, Magnetohydrodynamic (MHD) three-dimensional flow of second grade nanofluid by a convectively heated exponentially stretching surface, J. Mol. Liq., 220 (2016) 1004-1012.
[14] M. M. Rashidi, T. Hayat, E. Erfani, S.A.M. Pour and A. A. Hendi, Simultaneous effects of partial slip and thermal-diffusion and diffusion-thermo on steady MHD convective flow due to a rotating disk, Comm. Nonl. Sci. Numer. Simulation, 16 (2011) 4303-4317.
[15] C. Y. Cheng, Soret and Dufour effects on mixed convection heat and mass transfer from a vertical wedge in a porous medium with constant wall temperature and concentration, Trnsp. Porous Med., 94 (2012) 123--132
[16] M. Turkyilmazoglu and I. Pop, Soret and heat source effects on the unsteady radiative MHD free convection flow from an impulsively started infinite vertical plate, Int. J. Heat Mass Transfer, 55 (2012) 7635-7644.
[17] T. Hayat, M.I. Khan, M. Waqas and A. Alsaedi, Stagnation point flow of hyperbolic tangent fluid with Soret-Dufour effects, Results Phys., 7 (2017) 2711-2717.
[18] T. Hayat, I. Ullah, T. Muhammad and A. Alsaedi, Radiative three-dimensional flow with Soret and Dufour effects, Int. J. Mech. Sci., 133 (2017) 829-837.
[19] M. Turkyilmazoglu, The analytical solution of mixed convection heat transfer and fluid flow of a MHD viscoelastic fluid over a permeable stretching surface, Int. J. Mech. Sci., 77 (2013) 263-268.
[20] T. Grosan, J. H. Merkin and I. Pop, Mixed convection boundary-layer flow on a horizontal flat surface with a convective boundary condition, Meccanica, 48 (2013) 2149-2158.
[21] S. Das, R.N. Jana and O.D Makinde, Magnetohydrodynamic mixed convective slip flow over an inclined porous plate with viscous dissipation and Joule heating, Alex. Eng. J., 54 (2015) 251--61.
[22] M. Imtaiz, T. Hayat, M. Hussain, S.A. Shehzad G.Q. Chen and B. Ahmad, Mixed convection flow of nanofluid with Newtonian heating, Eur. Phys. J. Plus, 129 (2014) 97.
[23] T. Hayat, I. Ullah, A. Alsaedi, M. Waqas and B. Ahmad, Three-dimensional mixed convection flow of Sisko nanoliquid, Int. J. Mech. Sci., 133 (2017) 273-282.
[24] L. Zheng, C. Zhang, X. Zhang and J. Zhang, Flow and radiation heat transfer of a nanofluid over a stretching sheet with velocity slip and temperature jump in porous medium,

J. Franklin. Inst., 350 (2013) 990--1007.

[25] M. Sheikholeslami, D.D. Ganji, M.Y. Javed and R. Ellahi, Effect of thermal radiation on magnetohydrodynamics nanofluid flow and heat transfer by means of two phase model, J. Magn. Magn. Mater., 374 (2015) 36--43.

[26] F.M. Abbasi, S.A. Shehzad, T. Hayat and M.S. Alhuthali, Mixed convection flow of jeffrey nanofluid with thermal radiation and double stratification, J. Hydrodynamics Ser. B, 28 (2016) 840-849.

[27] T. Hayat, I. Ullah, B. Ahmed and A. Alsaedi, MHD mixed convection flow of third grade liquid subject to non-linear thermal radiation and convective condition, Results Phys., 7 (2017) 2804--2811.

[28] T. Hayat, I. Ullah, A. Alsaedi and B. Ahmad, Simultaneous effects of non-linear mixed convection and radiative flow due to Riga-plate with double stratification, J. Heat Transfer, 140 (2018) 102008.

[29] A.M. Salem and M.A. El-Aziz, MHD mixed convection and mass transfer from a vertical stretching sheet with diffusion of chemically reactive species and space or temperature-dependent heat source, Can. J. Phys., 85 (2007) 359-73.

[30] B. Mahanthesh, B.J. Gireesha and C.S.K. Raju, Cattaneo-Christov heat flux on UCM nanofluid flow across a melting surface with double stratification and exponential space dependent internal heat source, Informatics in Medicine Unlocked, 9 (2017) 26-34.

[31] Q.M. Zaigham Zia, I. Ullah, M. Waqas, A. Alsaedi and T. Hayat, Cross diffusion and exponential space dependent heat source impacts in radiated three-dimensional (3D) flow of Casson fluid by heated surface, Results Phys., 8 (2018) 1275-1282.

[32] S.J. Liao, On the homotopy analysis method for nonlinear problems, Appl. Math. Comput., 147 (2004) 499-513.

[33] M. Dehghan, J. Manafian and A. Saadatmandi, Solving nonlinear fractional partial differential equations using the homotopy analysis method, Numer. Meth. Partial Diff. Eq., 26 (2010) 448-479.

[34] V. Bansod and R. Jadhav, Effect of double stratification on mixed convection heat and mass transfer from a vertical surface in a fluid-saturated porous medium, Heat Transfer Asian Res., 39 (2010) 378-395.

[35] T. Hayat , I. Ullah, M. Waqas and A. Alsaedi, MHD stratified nanofluid flow by slandering surface, Phys. Scr., (2018),Doi.org/10.1088/1402-4896/aae1a2.

[36] S. Abbasbandy, T. Hayat, A. Alsaedi and M. M. Rashidi, Numerical and analytical solutions for Falkner-Skan flow of MHD Oldroyd-B fluid, Int. J. Numer. Methods Heat Fluid Flow, 24 (2014) 390-401.

[37] T. Hayat, I. Ullah, A. Alsaedi and Bashir Ahmad, Impact of temperature dependent heat source and nonlinear radiative flow of third grade fluid with chemical aspects, Therm. sci, (2018), DOI: 10.2298/TSCI180409245H.

[38] R. Ellahi, M. Hassan and A. Zeeshan, Shape effects of nanosize particles in $Cu-H_2O$ nanofluid on entropy generation, Int. J. Heat Mass Transfer, 81 (2015) 449-456.

[39] T. Hayat, I. Ullah, A. Alsaedi and M. Waqas, Double stratified flow of nanofluid subject to temperature based thermal conductivity and heat source, Therm. sci., (2018) DOI: 10.2298/TSCI180121242H.

[40] M. Turkyilmazoglu, An effective approach for evaluation of the optimal convergence control parameter in the homotopy analysis method, Filomat, 30 (2016) 1633-1650.

[41] T. Hayat, I. Ullah, T. Muhammad and A. Alsaedi, A revised model for stretched flow of

third grade fluid subject to magneto nanoparticles and convective condition, J. Mol. Liq., 230 (2017) 608-615.
[42] I. Ahmad, T. Javed, T. Hayat and M. Sajid, Series solutions for the radiation-conduction interaction on unsteady MHD flow, J. Porous Media, 14 (2011) 927-941.
[43] I. Ullah, M. Waqas, T. Hayat, A. Alsaedi and M. I. Khan, Thermally radiated squeezed flow of magneto-nanofluid between two parallel disks with chemical reaction, J. Therm. Anal. Calorim., (2018) Doi.org/10.1007/s10973-018-7482-6.